Nuclear Lamins A and B1: Different Pathways of Assembly during Nuclear Envelope Formation in Living Cells

Robert D. Moir, Miri Yoon, Satya Khuon, and Robert D. Goldman

Department of Cell and Molecular Biology, Northwestern University Medical School, Chicago, Illinois 60611

Abstract. At the end of mitosis, the nuclear lamins assemble to form the nuclear lamina during nuclear envelope formation in daughter cells. We have fused A- and B-type nuclear lamins to the green fluorescent protein to study this process in living cells. The results reveal that the A- and B-type lamins exhibit different pathways of assembly. In the early stages of mitosis, both lamins are distributed throughout the cytoplasm in a diffusible (nonpolymerized) state, as demonstrated by fluorescence recovery after photobleaching (FRAP). During the anaphase-telophase transition, lamin B1 begins to become concentrated at the surface of the chromosomes. As the chromosomes reach the spindle poles, virtually all of the detectable lamin B1 has accumulated at their surfaces. Subsequently, this lamin rapidly encloses the entire perimeter of the region containing decondensing chromosomes in each daughter cell. By this time, lamin B1 has assembled into a relatively stable polymer, as indicated by FRAP analyses and insolubility in detergent/high ionic strength solutions. In contrast, the association of lamin A with the nucleus begins only after the major components of the nuclear envelope including pore complexes are assembled in daughter cells. Initially, lamin A is found in an unpolymerized state throughout the nucleoplasm of daughter cell nuclei in early G1 and only gradually becomes incorporated into the peripheral lamina during the first few hours of this stage of the cell cycle. In later stages of G1, FRAP analyses suggest that both green fluorescent protein lamins A and B1 form higher order polymers throughout interphase nuclei.

Key words: nuclear envelope • mitosis • chromatin • intermediate filaments • green fluorescent protein

Introduction

The nuclear lamins are closely related to cytoplasmic intermediate filaments (IFs)[1] and are classified as Type V IF proteins (Moir et al., 1995; Stuurman et al., 1998). The lamins are the major components of the nuclear lamina, a fibrous structure adjacent to the nucleoplasmic face of the nuclear membrane. The lamina is required for maintaining nuclear size and shape, and may also play a role in the organization of chromatin. In addition, the lamins form structures within the nucleoplasm that are distinct from the peripheral lamina. These include lamin foci that are associated with sites of DNA replication (Goldman et al., 1992; Bridger et al., 1993; Moir et al., 1994).

The lamin family of proteins is classified into Types A and B based primarily on their amino acid sequence and their expression patterns. In vivo, B-type lamins are expressed in all cells, while A-type lamins are expressed only in differentiated cells (Benavente et al., 1985; Stewart and Burke, 1987; Rober et al., 1989). There are two B-type lamins in somatic cells, B1 and B2, that are products of different genes (Hoger et al., 1990; Zewe et al., 1991). In most mammalian somatic cells, the A-type lamins include lamins A and C, produced by differential splicing of the same gene (McKeon et al., 1986; Fisher et al., 1986). During mitosis, there is evidence that lamin B isotypes remain associated with membranes when the nuclear envelope is broken down and therefore have different biochemical properties when compared with A-type lamins (Gerace and Blobel, 1980).

As is the case for cytoplasmic IFs, the nuclear lamins have a central rod domain distinguished by heptad repeats characteristic of an alpha-helical structure. This rod domain is responsible for the dimerization of the lamin polypeptide chains and is also required for higher order interactions of the lamin dimers into the polymerized structures that form the nuclear lamina (Stuurman et al., 1998). The lamins have a short NH_2-terminal non–α-helical domain that is also essential for assembly (Moir et al., 1991; Heitlinger et al., 1992). The COOH-terminal domain includes the nuclear localization sequence (NLS) as well as

Address correspondence to Robert D. Goldman, Department of Cell and Molecular Biology, Northwestern University Medical School, 303 East Chicago Avenue, Chicago, IL 60611. Tel.: (312) 503-4215. Fax: (312) 503-0954. E-mail: r-goldman@northwestern.edu

[1]*Abbreviations used in this paper:* FRAP, fluorescence recovery after photobleaching; FRET, fluorescence energy transfer experiments; GFP, green fluorescent protein; IF, intermediate filament; LAP, lamin-associated protein; LBR, lamin B receptor; NLS, nuclear localization sequence.

a recognition sequence for isoprenylation (CAAX sequence), thought to be required for proper targeting of lamins A and B into the nucleus and the nuclear envelope, respectively (McKeon et al., 1986; Fisher et al., 1986; Loewinger and McKeon, 1988; Vorburger et al., 1989; Holtz et al., 1989). In addition, there is evidence that lamins A and C have chromatin-binding domains based upon in vitro assays (Hoger et al., 1991; Glass et al., 1993).

During interphase, the lamina plays an essential role in maintaining the shape and stability of the nuclear envelope (Newport et al., 1990; Spann et al., 1997). In support of this, nuclei are very fragile when assembled in *Xenopus laevis* egg extracts from which the majority of lamins have been immunodepleted or in which the lamina has been disrupted with a dominant-negative mutant (Newport et al., 1990; Spann et al., 1997). Furthermore, DNA replication is inhibited in lamin-depleted or -disrupted nuclei (Newport et al., 1990; Meier et al., 1991; Ellis et al., 1997; Spann et al., 1997; Moir et al., 2000). When the assembly of the lamina is disrupted with a dominant-negative lamin mutant, the endogenous lamins form aggregates within nuclei and the replication factors PCNA and RFC colocalize with these aggregates (Spann et al., 1997). This result suggests that lamins are required for the elongation phase of DNA replication and is in agreement with the observation that lamin B and PCNA colocalize in nucleoplasmic foci during S phase in cultured mammalian cells (Moir et al., 1994).

After mitosis, the assembly of the lamins into a lamina takes place during the formation of the nuclear envelope in daughter cells. However, the steps involved in this assembly process and the molecular interactions of the lamins with other envelope components have yet to be defined. The role of the lamins in nuclear assembly has been tested using in vitro nuclear assembly systems and the results are conflicting (Gant and Wilson, 1997). For example, if a lamin antibody is added to *Xenopus laevis* interphase extracts to block lamin function, nuclear assembly does not take place in the presence of chromatin (Dabauvalle et al., 1991). Instead, large aggregates, resembling annulate lamellae and containing nuclear pore intermediates, assemble in the extract. Similar results have been reported after the addition of lamin antibodies to nuclear assembly extracts derived from *Drosophila melanogaster* embryos or when lamins are immunoprecipitated from these extracts (Ulitzur et al., 1992, 1997). Furthermore, when lamins are immunodepleted from nuclear assembly extracts from mammalian cells, nuclear envelopes do not assemble properly around chromatin templates (Burke and Gerace, 1986). In addition, the reduced expression of lamins due to partial insertional inactivation of a *D. melanogaster* lamin gene results in defects of nuclear envelope structure in cells of affected flies, including the formation of annulate lamellae-like structures in the cytoplasm (Lenz-Bohme et al., 1997). Finally, in some systems, a fraction of the nuclear lamins appears to bind to chromatin very early in the process of nuclear formation, as seen in immunofluorescence assays (Yang et al., 1997). These results suggest that the lamins are required for successful envelope assembly (Foisner, 1997).

In contrast, other experiments show that intact nuclear envelopes assemble around chromatin after the immunodepletion of lamins from *X. laevis* interphase extracts (Newport et al., 1990; Meier et al., 1991). Furthermore, scanning electron microscopic studies of assembling nuclei in normal *Xenopus* extracts suggest that the lamins accumulate after membrane/pore complexes form (Wiese et al., 1997). Finally, other immunofluorescence observations of fixed mammalian cells undergoing nuclear assembly have suggested that the lamina is assembled after the nuclear membrane and nuclear pores have been established (Chaudhary and Courvalin, 1993). These results suggest that the lamins are imported into the nucleus and assemble only after the nuclear membrane and pore complexes have formed and, therefore, do not play a role in the initiation of envelope assembly (Newport et al., 1990). The apparent contradictions of the immunodepletion results obtained from different laboratories appear to be related to the inefficiency of this method for removing lamins from nuclear assembly extracts. In support of this contention, it has been shown that small amounts of lamins remain after immunoprecipitation, which appear to be adequate for the initiation of nuclear envelope assembly (Lourim and Krohne, 1993a,b).

To address the role of the lamins in nuclear assembly after mitosis and entry into the G1 phase of the cell cycle, we have expressed green fluorescent protein (GFP)–lamin fusion proteins in cultured cells. The utility of this approach for studying the lamins has already been demonstrated for the A-type lamins (lamins A, AΔ10, and C) by Broers et al. (1999). All three of these constructs are correctly processed and incorporated into the lamina of living interphase CHO-K1 cells. This work primarily describes several interphase structures that are revealed by GFP-lamin proteins. These include an extensive system of intra- and transnuclear tubular structures throughout the interphase nucleus. From fluorescence recovery after photobleaching experiments, the authors concluded that the tubules as well as the lamina exhibit relatively slow subunit exchange. In contrast, a second interphase population has an even distribution throughout the nucleoplasm, but appears to be much more diffusible, as demonstrated by fluorescence recovery after photobleaching (FRAP) experiments. The authors also showed that lamin A is dispersed throughout the cytoplasm in metaphase and enters daughter cell nuclei in late cytokinesis.

In this study, we describe in detail the dynamic properties of both A- and B-type lamins from metaphase through nuclear assembly and into G1. We chose to focus on this period of the cell cycle, because the role of the lamins in nuclear assembly remains controversial, as described above. The use of GFP-lamins allows us to determine the temporal sequence of changes in the distribution and the assembly state of the lamins in living cells during a time when they undergo profound changes in their structure and assembly states. To this end, the fates of lamins A, B1 and C during mitosis and nuclear envelope assembly in daughter cells were examined in vivo. The results demonstrate that there are significant differences between the A- and B-type lamins during nuclear assembly after mitosis. Lamin B1 begins to associate with chromatin in anaphase/telophase as chromosomes reach the spindle poles in daughter cells and before some nuclear pore components can be detected. Therefore, it appears that lamin B plays an early role in the assembly of the nuclear envelope. In contrast, lamin A does not obviously become associated

with chromosomes until after they have initiated the decondensation process in late telophase/mid-late cytokinesis. Furthermore, lamin B1 rapidly assembles into a relatively stable polymer as soon as it encloses the decondensing chromosomes in late telophase, as shown by FRAP, while lamin A is not incorporated into a stable structure in the peripheral lamina until much later in G1.

Materials and Methods

GFP-Lamin Constructs

The cDNAs for full-length human lamins A, B1, and C were cloned into the commercial GFP vector pEGFP-C1 (CLONTECH Laboratories, Inc.) (McKeon et al., 1986; Pollard et al., 1990) so that the GFP sequence was at the NH_2 terminus of the lamin sequence. For lamin A, a BamHI-EcoRI fragment containing the entire coding sequence of prelamin A (Weber et al., 1989), as well as the 11 amino acid myc 9E10 epitope at the NH_2 terminus (Evan et al., 1985) and a four amino acid linker, was cloned into the BglII-EcoRI site of pEGFP-C1. The human lamin C cDNA was cloned in an identical manner as lamin A. For lamin B1, a BamHI-EcoRI containing the entire coding region with a four amino acid linker was cloned into the BglII-EcoRI site of pEGFP-C1. In addition, lamin B1 was cloned into the cyan version of GFP (pECFP-C1; CLONTECH Laboratories, Inc.), and lamin A was cloned into the yellow version (pYFP-C1; CLONTECH Laboratories, Inc.) using the same strategy as was used for pEGFP-C1.

DNA sequences encoding only the COOH-terminal non–α-helical domain of lamin B1 were made by PCR using the full-length cDNA as a template. This construct encompassed residues 378–586 of the B1 sequence (LBT; Pollard et al., 1990). BamHI restriction enzyme sites were placed in the oligonucleotides used for the PCR to allow cloning of the fragments into pEGFP-C1. All mutant constructs were sequenced in their entirety using an ABI377 automated sequencer. Plasmids were purified by chromatography on QIAGEN columns or by CsCl gradient centrifugation.

Cell Culture and Transfection

An embryonic mouse epidermal cell line, PAM, was grown in DME with 10% fetal calf serum and antibiotics (100 μg/ml penicillin and streptomycin; Jones et al., 1982). The hamster kidney fibroblast line, BHK-21, was grown in DME containing 10% calf serum, antibiotics, and 10% tryptose phosphate broth, as previously described (Yoon et al., 1998).

The GFP-lamin fusion constructs were introduced into cells by electroporation. Cells at 50–80% confluency (~2–3 × 10^6 cells) were detached by trypsin treatment and resuspended in medium with 10 mM Hepes, pH 7.0. The cells were mixed with 7 μg of the GFP plasmid and 13 μg of carrier DNA (sonicated salmon sperm DNA; a gift of Dr. Sui Huang, Northwestern University, Evanston, IL) in an electroporation cuvette (BTX Inc.). An electroporator (Bio-Rad Laboratories) was used to deliver a pulse at 0.26 kV and 960 μF. The cells were plated onto 22-mm^2 No. 1 coverslips or onto dishes designed for use with the microscope stage temperature control system (Bioptechs). The transfection efficiency varied from 20 to 70%, depending on the construct used.

Microscopic Observations of Live Cells

Cells that had been transfected for 16–48 h were examined directly, or in some cases the cells were trypsinized and replated on standard or locator (Bellco Inc.) coverslips before examination 16–48 h later. For microscopic observations, the cells were transferred into Leibovitz's L15 medium containing 10% fetal calf serum and 100 μg/ml penicillin and streptomycin. The coverslips were mounted onto glass slides using chips of cover glass as feet to prevent compression and sealed with a mixture of lanolin, beeswax, and vaseline (1:1:1). The cells were maintained at 37°C while on the microscope stage using an airstream stage incubator (ASI400; Nevtek). In some cases, cells were examined in Bioptechs dishes using the Bioptechs stage/objective temperature controller.

Most time-lapse observations of GFP-transfected cells were made with an LSM 410 confocal microscope (Carl Zeiss Inc.) equipped with a 100× 1.3 NA oil immersion objective and an FITC filter set (excitation 488 nm, emission 515 nm). The observations relating to extraction of samples on the microscope were done using a 40× 1.0 NA oil immersion lens. Images were collected at time intervals using LSM software (Carl Zeiss Inc.). To minimize phototoxicity, the laser was set at 10–25% of full power and attenuated at 10 or 30%. Phase contrast was used to identify mitotic stages. In addition, an LSM 510 was used to image pCFP-lamin B1 and pYFP-lamin A simultaneously in doubly transfected cells. The 458- and 514-nm lines of the argon laser were used at 25–50% power for CFP and YFP respectively. The appropriate emission filters were obtained from Chroma.

FRAP was carried out as previously described (Yoon et al., 1998). In brief, bar-shaped regions were bleached using the line-scan function of the LSM 410 for 3–4 s at 488 nm with the laser set at 100% power with 1% attenuation. Fluorescence recovery was monitored by taking images at time intervals using 15% laser power with 10% attenuation. The time required for 50% recovery of the bleach zone ($t_{1/2}$) fluorescence was calculated using Metamorph imaging software as described previously (Yoon et al., 1998). In brief, the average fluorescence intensity (pixel value) of each postbleach image was equalized to that of the prebleach image to compensate for overall fading during image collection. A line along the bleached area of the lamina rim was drawn for each image using the line tool function of Metamorph and the profile of fluorescence intensity along the line determined using the line-scan function.

Fluorescence intensity was also measured using the Metamorph software. The average intensity of the background was subtracted from optical sections from the middle of the nucleus. Specific areas (lamina rim or nucleoplasm) of the image were selected with the Regions tool. The sum of the pixel values in these regions were used to determine total fluorescence intensity.

Fluorescence energy transfer experiments (FRET) were carried out on an Axiovert microscope (Carl Zeiss, Inc.) equipped with the appropriate filter sets. Cells doubly transfected with pCFP-LB1 and pYFP-LA were excited with light in the CFP excitation range (426–446 nm) and the emission was sequentially collected with CFP (455–485 nm) and YFP (520–550 nm) filter sets (Chroma) mounted on an external filter wheel. Subsequently, an image of YFP-LA was collected after excitation in the YFP excitation range. Images were collected with a 63× 1.4 NA oil immersion lens.

In some experiments, cells were extracted during microscopic observation. Transfected cells were plated into Bioptechs dishes as described above. Once a transfected cell was located, the culture medium was removed and IF extraction buffer (PBS containing 0.6 M KCl, 10 mM $MgCl_2$, and 1% Triton X-100) was added to the dish, taking care not to alter the position of the cell within the field of view. Image capturing was initiated immediately before extraction and within 10 s after the addition of the IF extraction buffer.

Indirect Immunofluorescence and Western Blotting

Cells on coverslips were washed with PBS, and then fixed with 4% formaldehyde in PBS for 10 min at room temperature. After fixation, the cells were permeabilized with 0.5% Triton X-100 in PBS for 5 min at room temperature, and then rinsed with PBS. The rabbit polyclonal antibodies for lamins A/C and B have been described previously (Moir et al., 1994). In addition, monoclonal antibodies directed against nucleoporins, mb414 (Babco) (Davis and Blobel, 1986), the nuclear pore protein NUP153 (a gift of Dr. Brian Burke, University of Calgary, Calgary, Alberta, Canada) (Bodoor et al., 1999), and lamin-associated protein 2β (LAP2β; a gift of Dr. Roland Foisner, University of Vienna, Vienna, Austria) (Dechat et al., 1998). A rabbit polyclonal antibody directed against LAP2β was also used in some studies (a gift of Dr. Kathy Wilson, Johns Hopkins University Medical School, Baltimore, MD) (Gant et al., 1999). Secondary antibodies consisted of lissamine rhodamine conjugated to donkey anti–rabbit IgG (Jackson ImmunoResearch Laboratories), fluorescein-conjugated goat anti–rabbit IgG and fluorescein-conjugated goat anti–mouse IgG (Molecular Probes). Fixed and stained cells were observed with either the LSM 410, LSM 510, or an Axiophot (Carl Zeiss, Inc.) equipped for epifluorescence. Images were recorded as previously described (Yoon et al., 1998).

Western blotting was performed as described in Yoon et al. (1998), except that chemiluminescence (Amersham Pharmacia Biotech) was used to detect the reactive products. The antibodies used were rabbit polyclonal antibodies to lamins A/C and lamins B1/B2 (Moir et al., 1994) or a monoclonal antibody to GFP (CLONTECH Laboratories, Inc.).

Results

The Assembly and Organizational States of Lamins during Cell Division

GFP human lamins A, B1, and C (see Materials and Methods) were transfected into either PAM or BHK-21 cells.

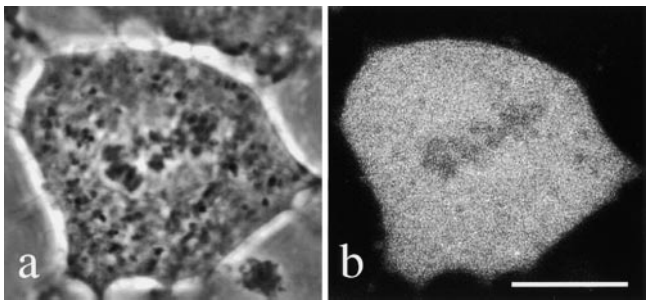

Figure 1. A live PAM cell in metaphase/early anaphase expressing GFP-lamin A observed by phase contrast (a) and fluorescence (b). The GFP-lamin signal fills the cytoplasm, but appears to be excluded from or greatly reduced in the area occupied by the chromosomes. The fluorescence image represents a single confocal section. Bar, 10 μm.

The expressed GFP fusion proteins were examined 16–48 h post-transfection by confocal or standard epifluorescence microscopy. Mitotic PAM cells retain the relatively flat appearance typical of dividing epithelial cells, making it easier to recognize each stage of mitosis. To determine the changes in lamin assembly states during these different stages, individual cells expressing GFP-lamins were followed from the metaphase/anaphase transition through cytokinesis and into G1 for several hours.

During metaphase, GFP-tagged lamins A, B1, and C are distributed diffusely throughout the cytoplasm, and are excluded only from the chromosome region (for example, Fig. 1). If photobleach zones are introduced into the cytoplasm at this stage, full fluorescence recovery takes place within a few seconds, before an image of the bleach zone can be obtained in a subsequent confocal laser scan (data not shown). This suggests that the lamins can move freely throughout the extrachromosomal cytoplasm.

Interestingly, there are temporal and organizational differences between B- and A-type lamins during the metaphase/anaphase transition through cytokinesis and into G1 (Fig. 2–4). In the case of lamin B1 in PAM cells (Fig. 2), the GFP signal intensifies in the peripheral region of chromosomes, mainly in the area closest to the spindle pole during mid to late telophase (Fig. 2, a and e). A few minutes later, as cleavage furrowing begins, the diffuse cytoplasmic fluorescence decreases, while the fluorescence intensity increases at the surface of the chromosomes. Within a short time, intense fluorescence is seen to completely enclose the decondensing chromosomes (Fig. 2, b and f). Lamin B1 always defines the perimeter of the decondensing chromatin as the nucleus grows during the transition from late cytokinesis into G1 (Fig. 2, c and g). At a slightly later stage, the cytoplasmic fluorescence is barely perceptible (Fig. 2, d and h). Similar patterns are seen when BHK-21 cells expressing GFP-lamin B1 are followed through mitosis (Fig. 3). However, in these cells, lamin B1 appears to accumulate at the surface of chromosomes in late anaphase or early telophase, which is earlier than seen in PAM cells. This accumulation, as indicated by

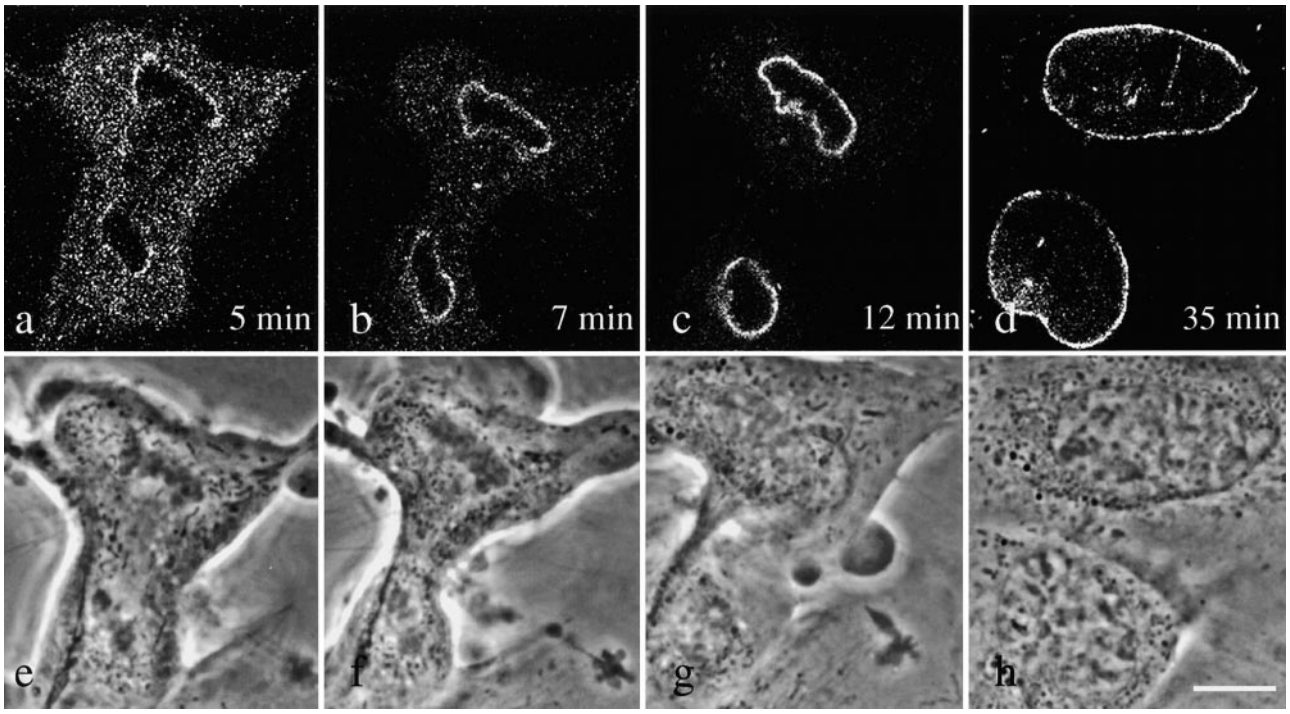

Figure 2. A series of confocal (a–d) and phase contrast (e–h) images of the same PAM cell expressing GFP-lamin B1 as it progresses from early telophase through nuclear assembly in daughter cells. The numbers in the lower right corner refer to the times after the metaphase to anaphase transition. (a and e) Increased fluorescence at the surface of the spindle pole side of the chromosome; (b and f) the same cell taken 2 min later, at which time lamin B1 appears to have completely enclosed the surface of the decondensing chromosomes in late telophase (note the overall reduction in cytoplasmic fluorescence); (c and g) 5 min later, showing that the vast majority of GFP-lamin B fluorescence is located at the surface the daughter cell nuclei, with almost no detectable cytoplasmic fluorescence; (d and h) the daughter cells ~30 min after the completion of telophase. Note the apparent increase in size of the nucleus. Bar, 10 μm.

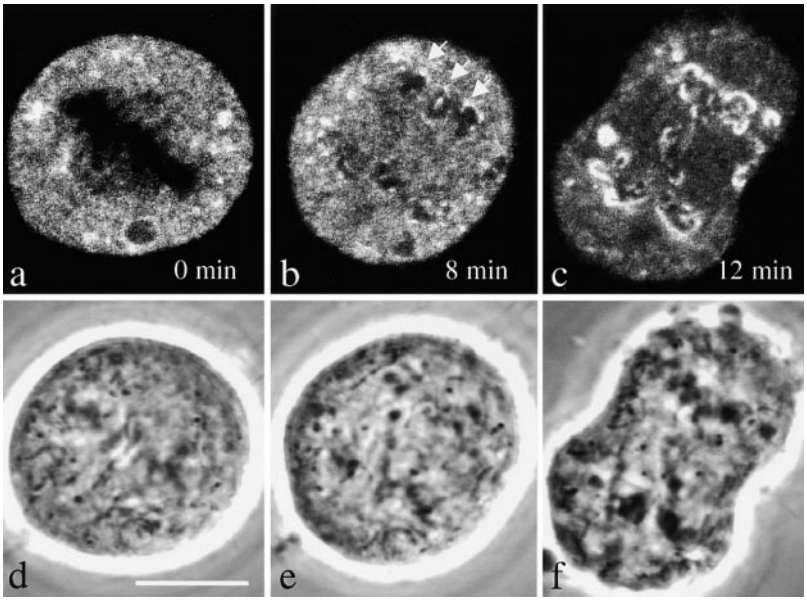

Figure 3. Confocal (a–c) and phase contrast (d–f) images of a live BHK-21 cell expressing GFP-lamin B as it progresses from metaphase to telophase. The first image is at metaphase/early anaphase and the subsequent images were taken 8 and 12 min later. Lamin B begins to associate with the surface of chromosomes in the region of the kinetochore facing the spindle poles by mid-late anaphase, 8 min later (b, arrows). This is most obvious in one set of chromosomes and not the other (bottom left) due to the fact that the spindle is slightly tilted. By the time of cleavage furrow initiation in mid-late telophase (4 min later), almost all detectable lamin B fluorescence is seen at the surface of the chromosomes that have reached the spindle poles (c, and f). Bar, 10 μm.

fluorescence intensity, is most obvious at the chromosome surface closest to the spindle poles (Fig. 3, a and d, and b and e). A few minutes later, as the chromosomes reach the poles and a cleavage furrow is initiated, the fluorescence intensity associated with surface of the chromosomes increases dramatically (Fig. 3, c and f). In addition, some bright lamin B1 foci can be seen in the cytoplasm of these cells throughout mitosis (Fig. 3, a–c). Similar cytoplasmic foci have been previously reported in dividing cells by indirect immunofluorescence (Chaudhary and Courvalin, 1993; Georgatos et al., 1997).

The organizational changes exhibited by GFP-lamin A are different from GFP-lamin B1 in PAM cells. Most obviously, lamin A initially accumulates throughout the region occupied by decondensing chromosomes in daughter cells (Fig. 4, a–f), rather than initially concentrating in the peripheral regions, as is the case for the B-type lamin. The lamin A fluorescence has a granular appearance during this time. Similar patterns of lamin A are seen in nontransfected PAM cells undergoing mitosis when examined by indirect immunofluorescence (compare Fig. 4, c with g). Cells expressing GFP-lamin C are indistinguishable from

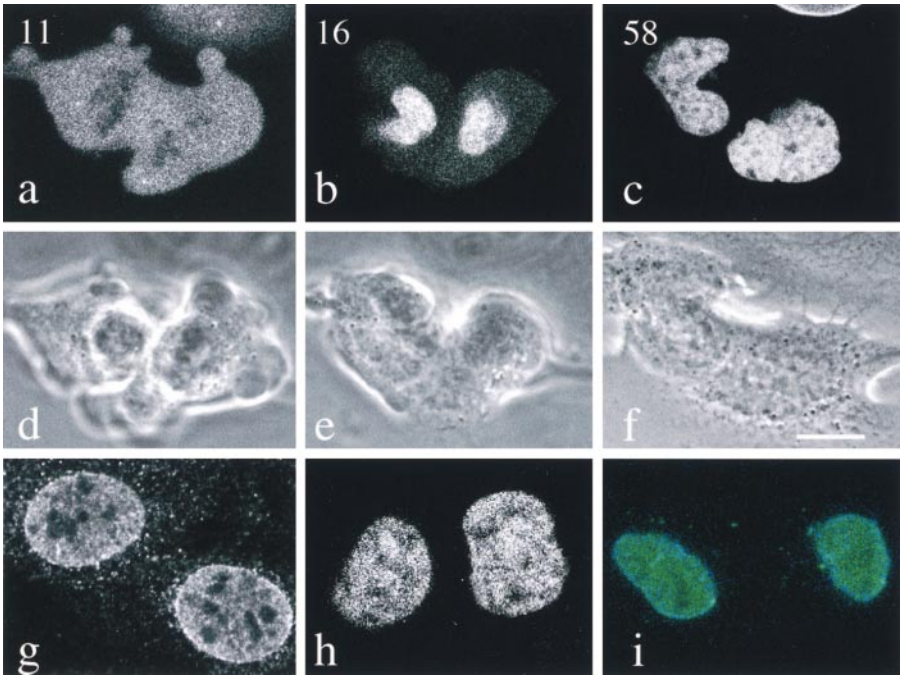

Figure 4. A series of confocal (a–c) and corresponding phase contrast (d–f) images of a live PAM cell expressing GFP-lamin A as it progresses from late telophase through early G1. The numbers in the top left hand corner refer to the times after the metaphase to anaphase transition. (a and b), In late telophase, lamin A remains uniformly distributed throughout the cytoplasm, except for the region containing the chromosomes. 5 min later (b and e), the majority of fluorescence is localized within daughter cell nuclei and the cytoplasmic fluorescence is greatly reduced. The overall pattern of nucleoplasmic fluorescence appears punctate. This pattern appears more obvious 58 min later in both daughter cells (c and f). Bar, 10 μm. Nontransfected PAM cells were fixed and prepared for indirect immunofluorescence with lamin A/C antibody. Early G1 daughter cells were identified by their overall morphology and the presence of a midbody using phase contrast (not shown). The confocal image of G1 cells shows primarily nucleoplasmic staining with relatively little lamin A/C staining in the cytoplasm or in the region of the nuclear lamina (g). GFP-lamin C shows a similar pattern as GFP-lamin A in early G1 (h, compare with c). The differences between B- and A-type lamins in early G1 distribution are seen in doubly transfected cells expressing CFP-laminB1 (blue) and YFP-laminA (green, i). Lamin A is found throughout the nucleoplasm and lamin B1 exclusively at the rim, but there is some overlap at the rim of the two proteins. Bars, 10 μm.

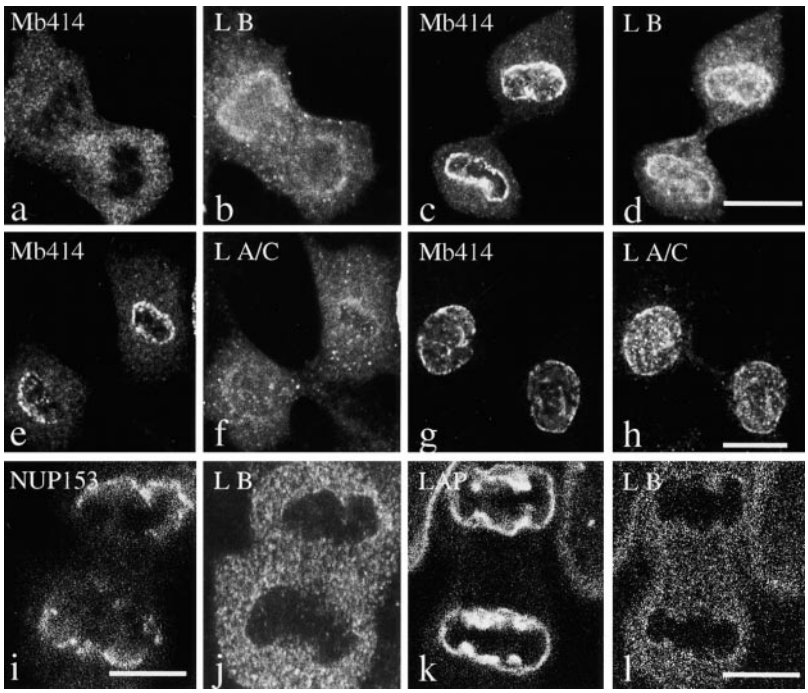

Figure 5. PAM cells fixed and prepared for double-label indirect immunofluorescence using antibodies against lamins B or A/C and nucleoporins (Mb414, a–h), NUP153 (i and j), and LAP2β (k and l). A cell in telophase is shown stained with Mb414 (a) and lamin B antibody (b). Lamin B accumulates first at the spindle side of chromosomes before the 414-reactive nucleoporins have begun to accumulate. By the late stages of cytokinesis (early G1), both nucleoporins (c) and lamin B (d) are mainly located in the peripheral region of daughter cell nuclei. In late cytokinesis/early G1, Mb414 stains primarily the peripheral region of daughter cell nuclei (e) and in the same cell the majority of lamin A/C appears distributed throughout the cytoplasm. Later in G1, nucleoporins (g) and lamin A/C (h) are found primarily in the nucleus. Cells in anaphase/telophase show staining at the spindle pole side with NUP153 (i) before lamin B (j). Similarly, LAP2β (k) has completely accumulated around chromatin before lamin B (l). All fluorescence images are confocal. Bars, 10 μm.

GFP-lamin A with respect to the lamin fluorescence after its accumulation in nuclei (compare Fig. 4, h with c). The different distributions of A- and B-type lamins immediately after nuclear assembly in early G1 are most clearly illustrated in cells expressing both pCFP-LB1 and pYFP-LA (Fig. 4 i). In this case, the lamin A signal is found throughout the nucleoplasm without an obvious concentration at the rim, and lamin B1 is found only at the periphery. However, the two proteins do overlap at the periphery (Fig. 4 i).

In addition, lamin A shows an association with chromatin at a later stage of cell division than does lamin B1. For example, lamin A fluorescence does not appear to become concentrated in the nuclear region until late cytokinesis as indicated by a well-developed cleavage furrow (11 min after metaphase/anaphase transition), after lamin B1 becomes associated with chromosomes (5–7 min after anaphase begins; compare Fig. 4, a and d, with 2, b and f, and 3, c and f).

The timing of the association of B- and A-type lamins with chromosomes was also compared with other components of the nuclear envelope. Nontransfected PAM cells were fixed and prepared for double indirect immunofluorescence with both a lamin B antibody that reacts with both lamins B1 and B2 (Moir et al., 1994) and an antibody that reacts with a set of five related nuclear pore components (mb414; Davis and Blobel, 1986). In telophase cells, when lamin B just begins to accumulate in the poleward region of chromosomes, no significant increase in nucleoporin staining is seen in association with these chromosomes (Fig. 5, a and b). At this stage, the nucleoporins appear to remain distributed throughout the cytoplasm. This suggests that lamin B becomes concentrated at the surface of chromosomes before some of the major nuclear pore components. At slightly later times, both lamin B and nucleoporin staining are concentrated in the peripheral region of the decondensing chromosomes (Fig. 5, c and d). Cells in the same stages of the cell division process were also double labeled with lamin A/C and the 414 antibody. In this case, the nucleoporin antibody became obviously concentrated at the perimeter of decondensing chromosomes before the lamin A/C antibody stained the chromosomal region (Fig. 5, e and f). At later times in G1, both lamins A/C and nucleoporins become concentrated in the nucleus (Fig. 5, g and h). Cells could not be found that showed increased lamin A/C staining in the nuclear region in the absence of nucleoporin staining during cell division and the early phases of G1.

These observations were extended using other nuclear pore and nuclear membrane markers. PAM cells were stained with both an antibody to the nuclear pore protein NUP153 (Bodoor et al., 1999) and the lamin B antibody. In contrast to the staining seen with the 414 antibody, NUP153 appears to become concentrated at the spindle pole side of the chromosomes before lamin B (Fig. 5, i and j). From these results, we infer the order of initial chromatin association to be NUP153, lamin B, 414-reactive nucleoporins, and lamin A/C. This is consistent with previous results suggesting sequential targeting of nuclear pore proteins (Bodoor et al., 1999; but see Haraguchi et al., 2000). In addition, the integral membrane protein LAP2β (Dechat et al., 1998) also appeared to aggregate around chromatin before lamin B, as suggested by immunofluorescence with lamin B and LAP2β antibodies (Fig. 5, k and l). In this case, LAP2β has almost completely accumulated around chromatin before lamin B. The nonmembrane-bound form of LAP2, LAP2α, showed similar staining (data not shown). We also did these experiments using the intrinsic GFP-laminB1 fluorescence, without antibody staining, in conjunction with the 414, NUP153, and LAP2 antibodies (data not shown) and obtained identical results.

Properties of Lamin B1 during Nuclear Assembly

To assess the state of lamin B1 polymerization during nuclear assembly, FRAP studies were carried out in trans-

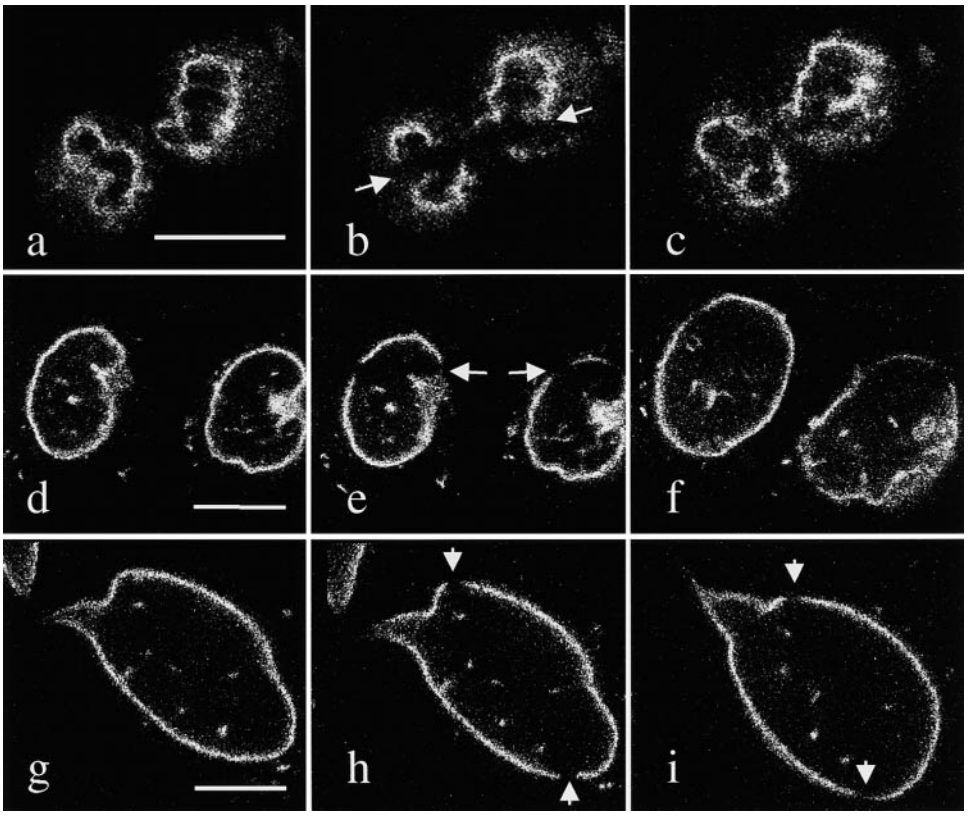

Figure 6. FRAP experiments were carried out on PAM cells expressing GFP-lamin B1 as nuclear assembly begins in late telophase and into G1. A bar-shaped bleach zone was made across the daughter cells and the recovery rate monitored in each of the forming nuclei. For each daughter cell, two bleach zones are introduced in the lamina rim. The recovery rate for each of these zones was estimated and averaged for each cell. For each time point, the prebleach image (a, d, and g), the immediate postbleach image (b, e, and h), and an image taken during the recovery period (c, f, and i) are shown. (a–c) The same nuclei before photobleaching at 10 min after lamin B enclosure (a), immediately after the introduction of a bleach zone (b, arrows), and 10 min after photobleaching (c), at which time the bleached area has almost completely recovered. (d–f) The same daughter cell nuclei immediately before photobleaching at 20 min after lamin B enclosure (d), immediately after photobleaching (e, arrows), and during recovery (f, 65 min after bleaching). During this period, daughter cell nuclei grew and tended to alter their positions slightly. (g–i) The same daughter cell nucleus at 45 min after lamin B enclosure (g), immediately after bleaching (h, arrows), and 180 min later (i, arrows). Only one daughter cell is shown due to the increase in nuclear size. After 180 min (i), the bleach zone shows only partial recovery (arrows). Bars, 10 μm (a–f) and 5 μm (g–i).

fected cells. Dividing cells in the metaphase-to-anaphase transition that had not yet shown an accumulation of GFP-lamin B1 at the surface of chromosomes (as indicated by an increase in fluorescence intensity) were identified and followed for up to 3 h into G1. At various times in the nuclear assembly process, bar-shaped bleach zones across entire nuclei were introduced in either one or both daughter cells. The rate of recovery for each bleach zone was monitored by capturing images at regular time intervals, and an average fluorescence recovery rate ($t_{1/2}$) was calculated for the bleach zone in the lamina rim. Typical results are illustrated in Fig. 6. For each FRAP experiment, three images are shown: images taken immediately before bleaching, immediately after bleaching, and an image taken during the recovery period. In Fig. 6, a–c, a bleach zone was introduced ~10 min after GFP-lamin B1 had first enclosed the decondensing chromosomes in daughter cells. The bleach zone appeared to recover completely within 10 min. This value is approximately the same as seen for normal vimentin IF in interphase (Yoon et al., 1998) and is also much greater than that seen for assembly-incompetent GFP-lamin B1 (see below). This suggests that lamin B1 starts to form a stable polymer almost immediately upon associating with the surface of the chromosomes. However, the FRAP rate was difficult to determine because nuclear shape, as defined by the peripheral lamin B1 fluorescent signal, was irregular and changed rapidly during the earliest stages of nuclear assembly. In general, nuclear shape appeared to stabilize within 20–30 min after lamin B1 enclosed chromatin, although the nuclear diameter continued to increase as cells progressed in G1. FRAP experiments during this time period gave a $t_{1/2}$ of 29 ± 15 min ($n = 8$; Fig. 6, d–f).

In FRAP studies carried out on daughter PAM cells 45–60 min after lamin B1 enclosure, recovery was very slow and bleach zones remained for more than 3 h into G1 (Fig. 6, g–i). We used the partial fluorescence recovery attained at the 3-h time point to estimate the $t_{1/2}$ to be ~120 ± 40 min ($n = 8$). This value suggests that lamin B1 has formed a polymer in the region of the lamina that undergoes relatively slow subunit exchange by this stage of G1. This slow recovery time of the peripheral lamina is similar to that seen in typical interphase cells chosen at random. In these cells, complete recovery of photobleach zones takes longer than 4 h (see Figs. 10, d–f, and 11), and the average $t_{1/2}$ appears to be >180 min (n = 3; Figs. 10 and 11). These FRAP experiments suggest that lamin B1 assembles into a relatively stable polymer rapidly after it associates with the surface of chromosomes in the late telophase/early G1 phases of the cell cycle.

As a further indicator of the state of polymerization of lamin B1 during nuclear assembly, and early G1, cells were extracted with a high salt/nonionic detergent buffer (IF buffer; see Materials and Methods) while being observed by confocal microscopy. This IF buffer has been used extensively to assess the polymeric state of IF proteins in cells (see Yoon et al., 1998). Individual transfected cells were identified in the metaphase/anaphase transition, followed

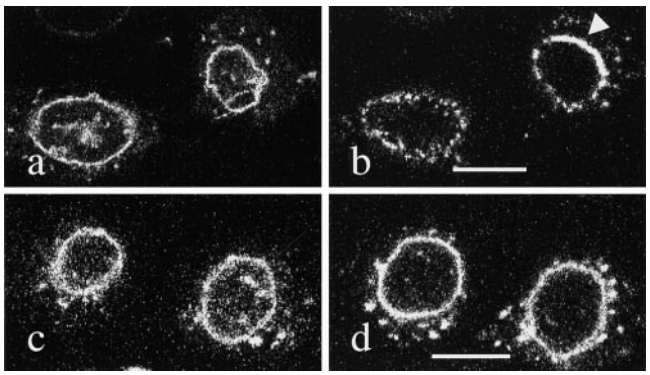

Figure 7. Confocal images of live PAM cells expressing GFP-lamin B1 before and after extraction with IF buffer. Cells were followed through nuclear assembly and at various time points, the culture medium was removed, and IF buffer was added. An image was collected ~10 s after extraction. A live cell 20 min after lamin B enclosure (a) and immediately after extraction (b). At this time point, the GFP-lamin B1 remaining after extraction consists of discontinuous spots and lines around the nucleus (arrow). A live cell was also followed for 45 min after enclosure (c), and then extracted with IF buffer (d). In this case, the GFP-lamin B forms an apparently continuous rim around the nucleus after extraction. In both cases (a and b, c and d), there are cytoplasmic lamin foci that have been reported by immunofluorescence in early G1 cells (Goldman et al., 1992; Chaudhary and Courvalin, 1993). Bar, 10 μm.

through lamin B1 enclosure of decondensing chromosomes and into the G1 phase. At different stages, the culture medium was removed and rapidly replaced with IF buffer on the microscope stage such that the same live cell could also be examined within 10 s after extraction (Fig. 7). When cells were extracted 10 min after enclosure of decondensing chromosomes in daughter cells, no remaining GFP-lamin B1 signal could be detected (data not shown). In daughter cells extracted 15–30 min after enclosure, some lamin B1 is removed or solubilized and the remaining lamin B1 is seen as an array of bright foci, or occasionally short lines, located at the nuclear periphery (Fig. 7 b, arrow). In contrast, the vast majority of GFP-lamin B1 remained as a continuous rim around the nucleus after extraction within 45–60 min after enclosure and in all typical interphase cells (Fig. 7, c and d). These results are in agreement with the results of the FRAP experiments, as they suggest that the formation of a stable lamin B1 polymer has occurred within the first 45–60 min after enclosure is initiated.

Lamin B1 Polymerization Is Required for Its Targeting and Stable Integration into the Lamina

To assess further the requirement for lamin B1 polymerization in lamina assembly during the earliest stages of nuclear assembly, PAM cells were also transfected with a GFP construct consisting only of the COOH-terminal domain of lamin B1 (termed LBT; amino acids 378–586). This fragment retains the NLS and the CAIM sequence (amino acids 583–586) that undergoes isoprenylation, but lacks the alpha-helical rod domain required for lamin polymerization. The NLS and CAIM motifs are required for proper lamin B targeting to the nuclear envelope (Loewinger and McKeon, 1988; Holtz et al., 1989; Kitten and Nigg, 1991; Frangioni and Neel, 1993; Hennekes and Nigg, 1994). Thus, this mutant lamin cannot polymerize independently or interact with endogenous lamins through rod domain, but it retains other sequences required for nuclear localization. When cells were examined within 20 min after the time when lamin B1 enclosure of chromatin normally takes place, the mutant protein appears to be dispersed throughout the nucleoplasm (Fig. 8 a). In contrast, wild-type lamin B1 is located almost exclusively at the nuclear periphery (Fig. 8 b). When bleach zones were introduced in cells expressing LBT at any stage of cell division or interphase, the fluorescence recovered before an image of the bleached area could be obtained in a subsequent confocal laser scan (<5 s). This suggests that the mutant protein is in a diffusible, nonpolymerized state (data not shown). In addition, the mutant protein can be completely extracted with IF buffer from early G1 cells, as well as cells at all other stages of the cell cycle (data not shown). These results further show that lamin B1 polymerization is a critical, early step in the establishment and maintenance of a stable nuclear lamina during nuclear envelope assembly after mitosis.

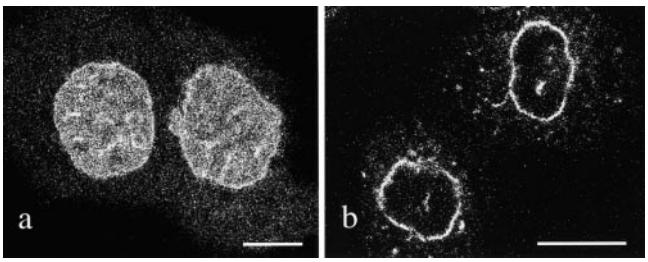

Figure 8. (a). A confocal image of live PAM daughter cells in early G1 (20 min after telophase) showing the expression pattern of the GFP–COOH-terminal fragment of lamin B1 that lacks the central rod assembly domain. The mutant lamin is relatively uniform in its distribution throughout the nucleoplasm. (b) In contrast, GFP–wild-type lamin B is mainly located in the lamina region of the daughter cell nuclei at ~20 min after telophase. Bar, 10 μm.

Lamin A follows a Different Pathway during Nuclear Assembly

Observations of lamin A during nuclear assembly in PAM cells indicate that it first accumulates throughout the region occupied by chromatin and is not immediately concentrated at the periphery (Fig. 4). This distribution is in contrast to that seen with lamin B1 (see above) and persists without evidence of a lamina rim pattern for ~60 min after GFP-lamin A begins to accumulate in assembling nuclei (Fig. 4 c). If live PAM cells showing this lamin A distribution are followed for an additional 90 min into G1, then the nucleoplasmic GFP-lamin A signal decreases as the lamina becomes more prominent at the nuclear periphery (Fig. 9, a and b). In addition, lamin foci become more obvious within the nucleoplasm (Fig. 9 b). We also observed a similar pattern of lamin A organization in BHK-21 cells (data not shown). GFP-lamin C shows an identical organization, including the presence of foci (data not shown).

FRAP experiments were carried out to assess the assembly state of lamin A during the transition from uniform nucleoplasmic fluorescence to a predominantly lamina rim pattern. Cells were first identified in stages ranging

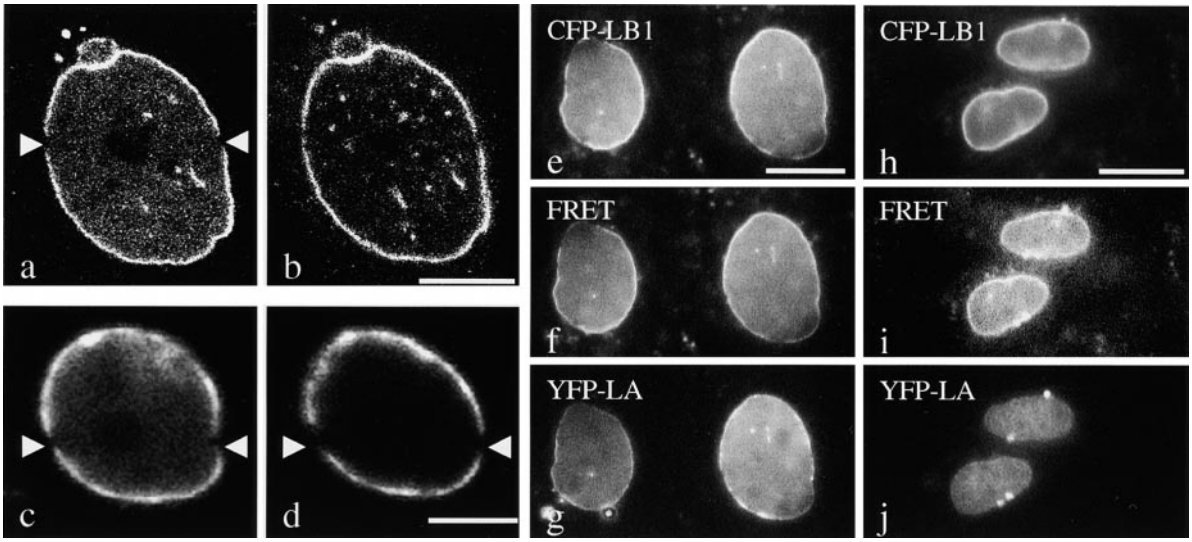

Figure 9. Mitotic PAM cells were identified and allowed to proceed until ~60–90 min after telophase. At this time, both the nucleoplasm and lamina fluoresce. When daughter cell nuclei are photobleached at this time, the recovery in the nucleoplasm is so fast that a bleach zone cannot be detected in a subsequent confocal scan (a). However, the bleached areas in the lamina region recover much more slowly and remain detectable for up to 70 min and later. Only one daughter cell nucleus is shown due to the size of the nucleus. The overall nucleoplasmic fluorescence becomes less intense during this period of observation and the number of nucleoplasmic foci increase. Many of these foci are not continuous with the nuclear surface, as shown through a focus series of images using the confocal microscope (not shown). Bar, 10 μm. A live PAM cell in early G1 expressing GFP-lamin A was photobleached across the entire cell and an image was captured in the subsequent confocal scan (d). As expected for an early G1 cell, the bleach zone is apparent only at the lamina rim (arrows). This same cell was immediately extracted in IF buffer while being viewed on the microscope stage and an image was captured 10-s later (e). The nucleoplasmic fluorescence is almost completely extracted. Bar, 5 μm. FRET analysis was also performed on cells in G1 (e–j). Cells were doubly transfected with pCFP-LB1 and pYFP-LA and examined using a FRET filter setup, as described in Materials and Methods. In cells early in G1 (120–180 min after telophase), the CFP-LB1 (e) was able to activate YFP-LA, resulting in a FRET signal (f), implying these molecules interact. Furthermore, cells very early in G1 (<90 min after telophase), when lamin A is largely nucleoplasmic (YFP-LA; j) also have a FRET signal, indicating an interaction at this time (h and i). Bar, 10 μm.

from telophase to early cytokinesis and followed for an additional 60–120 min as they entered the G1 stage. Bar-shaped bleach zones were made across the nuclei of one or both daughter cells at various time points. In early G1 nuclei containing both nucleoplasmic fluorescence and a distinct, more intensely fluorescent lamina region (60–120 min after cytokinesis), the bleach zone recovers immediately in the nucleoplasm, but much more slowly in the rim region (Fig. 9 a, arrows). The $t_{1/2}$ for fluorescence recovery in the rim during this period was 87 ± 25 min ($n = 4$). The nucleoplasmic foci seen in early G1 cells (Fig. 9 b) also show long photobleach recovery times, suggesting that they represent stable structures (data not shown). When early G1 cells were extracted with IF buffer, the diffuse nucleoplasmic fluorescence was greatly reduced, while the lamina signal remained intense and retained its photobleached zone (Fig. 9, c and d). The lamin foci were generally resistant to extraction.

To assess the possibility of interactions between lamins A and B1 during nuclear assembly, we performed FRET (Damelin and Silver, 2000) using the cyan (CFP) and yellow (YFP) versions of GFP. In this method, cells expressing CFP and YFP (see Materials and Methods) are exposed to light in the CFP excitation range (426–446 nm). The activated CFP (donor) emits energy that activates YFP molecules that are very close to CFP (<10 nm; Heim and Tsien, 1996). Images of the CFP and activated YFP (FRET image) were collected sequentially. An image of the YFP-LA excited independently at the YFP maxima (490–510 nm) was collected subsequently for comparison. In our experimental design, pCFP-LB1 acted as an energy donor to activate pYFP-LA. Cells in G1 were identified by the size of their nuclei and analyzed for FRET by conventional epifluorescence. As shown in Fig. 9, e–g, the CFP-LB1 activates YFP-LA, resulting in an image very similar to the CFP-LB1 alone in later G1 cells, identified as a pair of smaller nuclei (FRET image; Fig. 9, compare f with e). We also identified earlier G1 cells on basis of an apparent YFP-LA nucleoplasmic distribution (Fig. 9 j). In these cells, there is also a FRET signal when the CFP-LB1 is excited (Fig. 9, h and i). This suggests that lamins A and B1 interact at this earlier stage of G1. Although lamin A is not concentrated at the rim, there is apparently some overlap with lamin B1. CFP-LB1 and YFP-LA do not produce FRET images when transfected alone, indicating there is no bleedthrough in the emission or excitation filters (data not shown).

Evidence for a Nucleoplasmic Lamin Network in Interphase Cells

We noted that in addition to the dividing the cells that we followed into early G1 (see above), the majority of transfected interphase cells exhibited both GFP-lamins A and B1 fluorescence within the nucleoplasm, in addition to that found at the nuclear periphery. A typical example of this type of fluorescence pattern is seen in Fig. 10, a and d. This

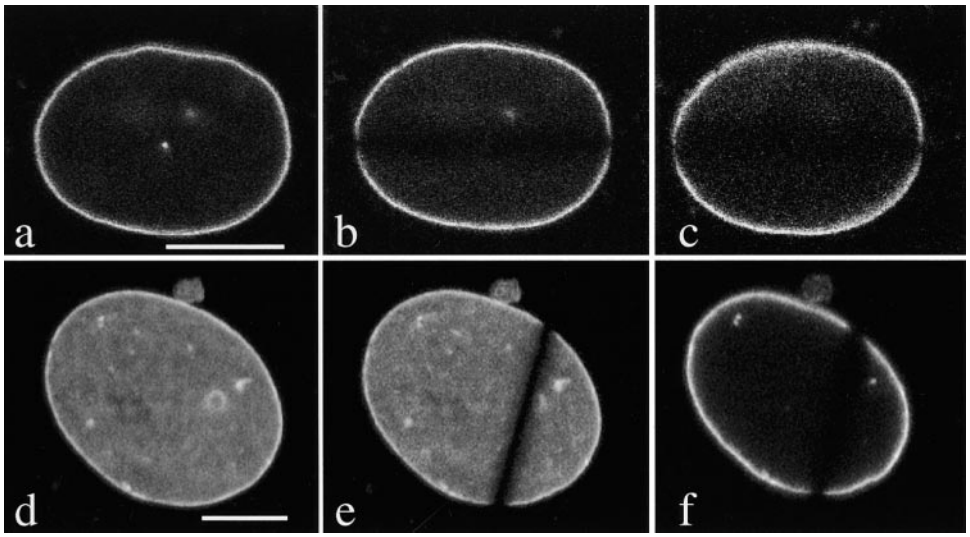

Figure 10. GFP-lamin A and B show intranuclear fluorescence in the majority of interphase PAM cells. (a–e) A live cell expressing GFP-lamin B shows nucleoplasmic (the lamin "veil") and lamina fluorescence (a) with confocal optics. In b, the cell was photobleached, and after 240 min (c) the bleach zone could still be detected. The $t_{1/2}$ for both the nucleoplasm and lamina is similar (~180 min, see text and Fig. 11). This veil can be seen throughout the nucleoplasm in a confocal through focus series (not shown). (d–f) Live PAM cells expressing GFP-lamin A have a more prominent nucleoplasmic veil. An optical section from an interphase cell expressing GFP-lamin A is shown just before (d), and just after (e) photobleaching. Note that the prominent bleach zone is retained across the entire nucleus, suggesting that this is not an early G1 cell (see text). In f, the same cell was extracted immediately after photobleaching with IF buffer and an image was captured. The veil fluorescence is greatly reduced, but lamina fluorescence appears unaltered. Bars, 10 μm.

pattern is seen with both GFP-lamin A and GFP-lamin B1. Of particular interest is a "veil" of fluorescence in the nucleoplasm (Fig. 10, a and d). This veil appears to fill the nucleoplasm and the region surrounded by the prominent lamina. Images obtained in through focus series show that this veil is present throughout the nucleus, but appears to be excluded from the nucleolus. A similar nucleoplasmic veil of fluorescence is seen in nontransfected cells observed by immunofluorescence with antibodies directed against lamins A and B (data not shown). We measured fluorescence intensity in the lamina rim and in the nucleoplasm using the Metamorph image analysis program. For interphase cells expressing GFP-lamin A, the lamina rim comprises 24% ($n = 5$) of the total intensity, while or GFP-laminB1 the rim forms 32% ($n = 5$) of the total.

When bleach zones are introduced across both the rim and the veil in interphase cells, the FRAP recovery rate is very slow for both of these structures (Fig. 11, b and e, >180 min, $n = 3$). This slow recovery rate suggests that the veil in these nuclei is composed of a stable lamin-containing structure. In the case of GFP-lamin A, this is distinct from that seen in early G1 (Fig. 9 a), at which time the recovery of nucleoplasmic fluorescence occurs immediately. However, when these interphase cells are extracted with IF buffer, the internal fluorescent signal is greatly diminished, although the lamina rim fluorescence is preserved (Fig. 10 f). In this latter experiment, a stable bleach zone has been introduced to make certain that the cell is not in early G1 (Fig. 10 e).

Although we clearly have established the presence of an internal lamin structure, it is possible that this structure results from overexpression and accumulation of the GFP fusion protein. We quantitated the relative amount of GFP fusion protein by performing Western blots with samples of transfected cell cultures using our lamin A/C or lamin B antibodies as probes. The GFP-lamin A and B fusion proteins are not detectable in a Western blot with these antibodies when the maximum amount of sample is loaded on the gel (30 μl). The endogenous proteins are detectable with as little as 10% of the same extract. Approximately 21% (LA) or 45% (LB) of the cells were transfected and we have estimated that fusion proteins are expressed at <47 and 21% of the endogenous proteins, respectively. This is similar to previous results with GFP-vimentin (Yoon et al., 1998) or when stable cell lines are made using GFP-lamins (Broers et al., 1999).

Discussion

In the work described here, GFP fusion proteins have been used to observe the dynamic properties of nuclear lamins during nuclear assembly in daughter cells. A recent report also described the properties of GFP lamin A fusion proteins, primarily in interphase nuclei (Broers et al., 1999). The results reported here describe for the first time the different pathways of assembly and the organization of A- and B-type lamins in living cells during mitosis, nuclear formation in daughter cells, and the G1 phase of the cell cycle.

When we follow cells expressing GFP-lamins, we observe that lamin B1 is targeted directly to the periphery of chromosomes before significant decondensation begins, and remains at the nuclear boundary. In contrast, lamin A is targeted to the nucleoplasm of newly formed nuclei and is not initially concentrated at the periphery of chromosomes. In PAM cells, lamin B1 begins the process of enclosure in telophase, as the chromosomes reach the spindle poles, before the decondensation process begins. In contrast, lamin A does not begin to associate with chromosomes until the late stages of cytokinesis after the decondensation process has been initiated. In BHK-21 cells, increased lamin B1 fluorescence is seen associated with chromosomes in mid-to-late anaphase/early telophase, earlier than seen in PAM cells. In both cell types, lamin B1 first accumulates on the spindle pole side of the chromosomes, in the region of the kinetochore, suggesting lamina assembly may be initiated at this site. Therefore, this may

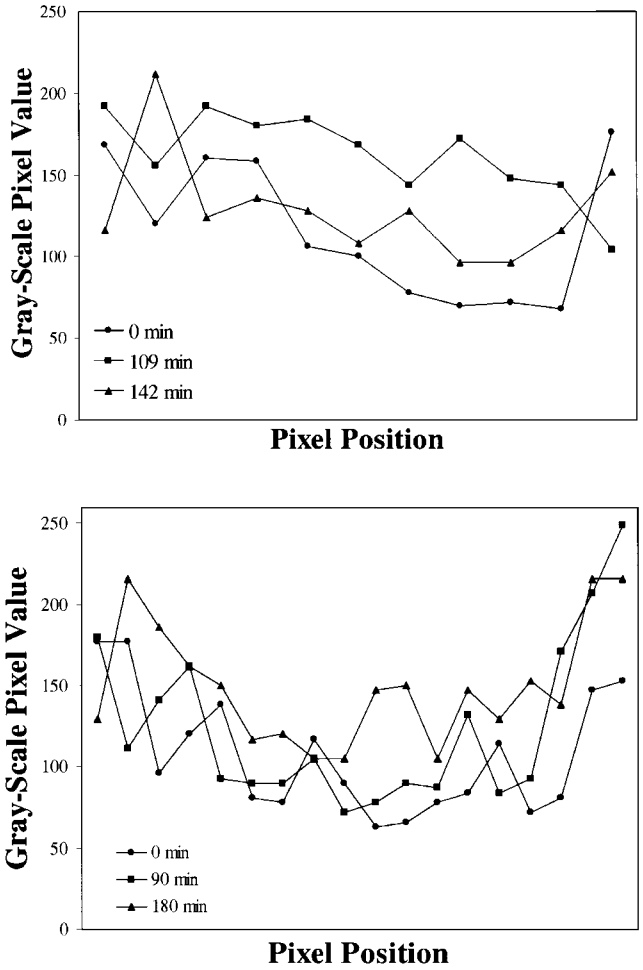

Figure 11. The fluorescence recovery rates for bleach zones in the lamina rim of interphase cells are shown as an X–Y plot of fluorescence intensity (pixel value) versus pixel position. The average fluorescence intensity (pixel value) of each postbleach image was equalized to that of the prebleach image to compensate for overall fading during image collection. A line along the bleached area of the lamina rim was drawn for each image using the line tool of the Metamorph image analysis program and the profile of fluorescence intensity along the line determined using the line-scan function. The profiles obtained from different time points were plotted and the bleach zone appears as a trough relative to adjacent unbleached areas. Fluorescence recovery was determined by measuring the relative fluorescence recovery in the bleached to the unbleached areas over time. (Top) Recovery for an interphase cell expressing GFP-lamin B1 in interphase. Approximately 50% recovery occurs in 142 min. (Bottom) A cell at interphase expressing GFP-lamin A. This bleach zone has undergone <50% recovery in 3 h.

also represent an early nucleating site for the assembly of the nuclear envelope. In support of this, lamin B1 targeting to the surface of chromosomes occurs before an obvious accumulation of some nuclear pore proteins, implying that lamin B1 assembly begins before pore assembly is completed. The results also show that lamin A is transported into the nucleus after the nucleoporins become associated with the surface of decondensing chromosomes, suggesting that lamin A requires functional nuclear pores to enter the nucleus. Our results on the timing of recruitment of nuclear envelope components are in agreement with results from fixed cells, which suggest sequential binding of different nuclear pore proteins to chromatin (Bodoor et al., 1999). However, a recent study in live cells indicates that NUP153, p62 (a 414-reactive protein), lamin B receptor (LBR), and emerin associate with chromosomes almost simultaneously in early telophase (Haraguchi et al., 2000). These results also show that LBR and emerin are initially punctate in their distribution around chromatin and do not become uniform until later in telophase. Therefore, it is tempting to speculate that the binding of lamin B1 that we detect at this same time in the cell division process is required to establish LBR and emerin distribution, through direct interactions or indirectly through the formation of a lamin polymer (see below).

Different patterns of A- and B-type lamins in telophase/early G1 have also been described in other cell types using immunofluorescence. For example, the same overall distributions have been reported for A- and B-type lamins in normal rat kidney cells during early G1 (Dechat et al., 1998). Nucleoplasmic staining with antibodies directed against lamin A/C has also been reported during early G1 in other cells (Goldman et al., 1992; Bridger et al., 1993; Hozak et al., 1995; Neri et al., 1999). In addition, the recent results with GFP-tagged lamins A, LAΔ10, and lamin C in CHO cells indicate that they exhibit a nucleoplasmic distribution during G1 (Broers et al., 1999).

In this study, we show that as cells progress through G1, lamins A and B1 exhibit significantly different assembly properties and locations. In the case of lamin B1, a higher order polymer is established rapidly at the nuclear periphery based on the fluorescence recovery rates of cells at this time in the cell cycle. At the earliest stages of lamin B1 enclosure around chromatin, photobleach zones recover in ~10 min. This value is similar to that obtained for polymerized interphase cytoskeletal IF networks (Vickstrom et al., 1992; Yoon et al., 1998) and suggests that lamin B1 is beginning to polymerize on the surface of decondensing chromosomes almost immediately after mitosis. FRAP rates increase in the first 60 min of G1, indicating that lamin B1 is rapidly assembled into a higher order structure after mitosis.

The importance of lamin B1 polymerization in the early stages of lamina assembly is also supported by the expression of the mutant protein, LBT. The absence of the alpha-helical rod prevents this mutant lamin from assembling the coiled-coil dimers required for the subsequent steps in lamin assembly, but it retains the NLS and isoprenylation sites required for nuclear targeting and nuclear membrane association (Peter et al., 1991). LBT remains distributed uniformly in the nucleoplasm throughout the cell cycle, and it does not appear to be targeted specifically to the lamina (see Fig. 8). Furthermore, FRAP analysis shows that this mutant protein remains in a diffusible state throughout the nucleoplasm, demonstrating that lamin B1 polymerization, in addition to the NLS and CAAX signals, is required to establish normal lamin B1 organization.

Lamin A exhibits dramatically different dynamic properties relative to lamin B1 during G1. Immediately after mitosis and into the early phase of G1, lamin A is distributed throughout the nucleoplasm of the assembling nucleus of both PAM and BHK cells. The fast fluorescence

recovery rates recorded at this time suggest that lamin A is present in a form that is more mobile and hence represents a lower order structure. For ~90–120 min after its initial targeting to the nucleoplasm, lamin A is gradually incorporated into the lamina, as shown by the shift in the intensity of the GFP-lamin A signal from the nucleoplasm to the nuclear periphery. During this time, lamin A exists in two populations with different polymeric states as shown by the FRAP rates and extraction properties.

The differences in lamins A and B1 distributions may reflect their different interactions with other nuclear envelope components. For example, it is known that B-type lamins are associated with nuclear envelope-derived membrane vesicles in mitotic cells (Gerace and Blobel, 1980; Burke and Gerace, 1986; Vigers and Lohka, 1991; Lourim and Krohne, 1993a; Meier and Georgatos, 1994; Foisner, 1997; Maison et al., 1997; Drummond et al., 1999). Therefore, lamin B1 would be expected to be localized peripherally during the early stages of assembly as part of the forming nuclear membrane. Furthermore, LAPs probably mediate the interactions of lamins with membranes (Foisner, 1997; Yang et al., 1997). The LAP family includes LAP2 α and β, emerin and MAN1 (Lin et al., 2000). In particular, LAP2 has been implicated in the regulation of the early stages of nuclear assembly and also in the growth of the nucleus during G1 (Yang et al., 1997; Dechat et al., 1998; Gant et al., 1999; Vlcek et al., 1999). Different fragments of LAP2 can inhibit either nuclear assembly or nuclear growth, perhaps reflecting the binding of this protein to chromatin or lamins (Yang et al., 1997; Gant et al., 1999). LAP2α, a non–membrane-bound isoform, colocalizes with A-type lamins during nuclear formation and may specifically regulate the assembly of lamin A (Dechat et al., 1998). Since LAP2β may interact primarily with lamin B isoforms, the distributions of lamins A and B1 that we observe may reflect interactions with different forms of LAP2 during nuclear assembly (Dechat et al., 1998). Furthermore, it has been proposed that the membrane-bound LBR interacts with lamin B only (Meier and Georgatos, 1994; Ellenberg et al., 1997; Drummond et al., 1999), although this putative lamin B-LBR interaction has been questioned (Mical and Monteiro, 1998; Gajewski and Krohne, 1999).

The different distributions of lamins A and B1 may also be due to posttranslational modifications. For example, lamins A and B are isoprenylated at a conserved COOH-terminal cysteine (Holtz et al., 1989; Kitten and Nigg, 1991). The isoprenyl group remains on lamin B throughout the cell cycle (Firmbach-Kraft and Stick, 1993, 1995), but it is rapidly removed from lamin A by an endoprotease (Weber et al., 1989; Kilic et al., 1999). The mutation of the cysteine residue prevents isoprenylation and results in an exclusively nucleoplasmic distribution of lamin A (Holtz et al., 1989). However, other experiments using inhibitors of isoprenylation suggest that lamin A incorporation into the lamina is not affected by the inhibition of this posttranslational event (Dalton et al., 1995; Sasseville and Raymond, 1995). In our studies, it is most likely that the majority of the lamin A that we observe localizing to the nucleus immediately after mitosis is synthesized in the previous cell cycle (Gerace et al., 1984) and therefore would not be isoprenylated as a consequence of the proteolytic cleavage step. It is possible, therefore, that as new, isoprenylated lamin A is synthesized during G1, it interacts, perhaps by forming dimers or tetramers, with the nucleoplasmic lamin A synthesized in the previous cell cycle, resulting in the targeting of both populations to the envelope.

We have also obtained evidence in this study that lamins A and B can exist in a polymerized state within the nucleoplasm in late G1 or other interphase stages, as a veil of fluorescence that is distinct from the peripheral lamina. Both the lamin A and B veils are distributed throughout the nucleus, as shown by through-focus series in the confocal microscope (data not shown). Furthermore, very slow FRAP rates were obtained for the A- and B-type veils, as well as the lamina. In the case of lamin A, this is contrasted with the extremely rapid fluorescence recovery obtained in early G1 cells. However, throughout interphase, the structure of the veil appears biochemically distinct from the lamina, as indicated by a significant reduction in fluorescence intensity after extraction with IF buffer. The recent report using GFP–A-type lamins in CHO cells also describes intranuclear fluorescence, although these workers report that fluorescence recovery takes only 1.5 s (Broers et al., 1999). This discrepancy with our results, especially in the later phases of G1, could be explained by the stage of the cell cycle during which FRAP experiments were carried out. In comparison with our data, the result of Broers et al. (1999) would be expected from early G1 cells. It will be an important priority, therefore, to determine the relationships of the different intranuclear lamin structures to each other during specific stages of the cell cycle.

There are now a number of reports of nucleoplasmic lamin structures in fixed, nontransfected cells (Hozak et al., 1995; Hozak, 1996; Neri et al., 1999). In support of this, immunoelectron microscopy of extracted, fixed cells has revealed putative lamin filaments within the nucleus (Hozak et al., 1995). We have also observed lamin staining within the nucleoplasm using immunoelectron microscopy (data not shown). Based on these considerations, it is interesting to consider the possibility that the nuclear lamins, as a member of the IF family of proteins, form the framework for an extended and pervasive nucleoskeletal system that is continuous with the lamina during interphase (Hozak et al., 1995). The detailed organization, state of polymerization, or structure of this lamin-based nucleoskeleton remains to be explored. However, its existence has profound implications for many nuclear functions (Pederson, 1998, 2000a,b). Among these are the determination of nuclear size, shape, mechanical properties, the organization of chromatin, and DNA replication. In support of the latter, it has been shown that lamin B colocalizes with DNA replication centers in situ (Moir et al., 1994), and there is a significant amount of evidence showing that an intact nuclear lamina is required for the completion of DNA replication (Newport et al., 1990; Spann et al., 1997; Ellis et al., 1997; Moir et al., 2000). Therefore, the existence of a dynamic nucleoplasmic lamin network may ultimately prove to represent the infrastructure required for many important nuclear functions.

We thank Drs. Brian Burke, Roland Foisner, Katherine Wilson, and Howard Worman for gifts of antibodies. We also thank Drs. Teng-Leong Chew and Rex Chisholm for the use of their FRET system.

This work was supported by grant CA31760 from the National Cancer Institute.

Submitted: 28 October 1999
Revised: 29 September 2000
Accepted: 6 October 2000

References

Benavente, R., G. Krohne, and W.W. Franke. 1985. Cell type-specific expression of nuclear lamina proteins during development of *Xenopus laevis*. *Cell.* 41:177–190.

Bodoor, K., S. Shaikh, D. Salina, W.H. Raharjo, R. Bastos, M. Lohka, and B. Burke. 1999. Sequential recruitment of NPC proteins to the nuclear periphery at the end of mitosis. *J. Cell Sci.* 112:2253–2264.

Bridger, J.M., I.R. Kill, M. O'Farrell, and C.J. Hutchison. 1993. Internal lamin structures within G1 nuclei of human dermal fibroblasts. *J. Cell Sci.* 104:297–306.

Broers, J.L., B.M. Machiels, G.J. van Eys, H.J. Kuijpers, E.M. Manders, R. van Driel, and F.C. Ramaekers. 1999. Dynamics of the nuclear lamina as monitored by GFP-tagged A-type lamins. *J. Cell Sci.* 112:3463–3475.

Burke, B., and L.A. Gerace. 1986. A cell free system to study reassembly of the nuclear envelope at the end of mitosis. *Cell.* 44:639–652.

Chaudhary, N., and J.-C. Courvalin. 1993. Stepwise reassembly of the nuclear envelope at the end of mitosis. *J. Cell Biol.* 122:295–306.

Dabauvalle, M.C., K. Loos, H. Merkert, and U. Scheer. 1991. Spontaneous assembly of pore complex-containing membranes ("annulate lamellae") in *Xenopus* egg extract in the absence of chromatin. *J. Cell Biol.* 112:1073–1082.

Dalton, M.B., K.S. Fantle, H.A. Bechtold, L. DeMaio, R.M. Evans, A. Krystosek, and M. Sinensky. 1995. The farnesyl protein transferase inhibitor BZA-5B blocks farnesylation of nuclear lamins and p21ras but does not affect their function or localization. *Cancer Res.* 55:3295–3304.

Damelin, M., and P.A. Silver. 2000. Mapping interactions between nuclear transport factors in living cells reveals pathways through the nuclear pore complex. *Mol. Cell.* 5:133–140.

Davis, L.I., and G. Blobel. 1986. Nuclear pore complex contains a family of glycoproteins that includes p62: glycosylation through a previously unidentified cellular pathway. *Proc. Natl. Acad. Sci. USA.* 84:7552–7556.

Dechat, T., J. Gotzmann, A. Stockinger, C.A. Harris, M.A. Talle, J.J. Siekierka, and R. Foisner. 1998. Detergent-salt resistance of LAP2alpha in interphase nuclei and phosphorylation-dependent association with chromosomes early in nuclear assembly implies functions in nuclear structure dynamics. *EMBO (Eur. Mol. Biol. Organ.) J.* 17:4887–4902.

Drummond, S., P. Ferrigno, C. Lyon, J. Murphy, M. Goldberg, T. Allen, C. Smythe, and C.J. Hutchison. 1999. Temporal differences in the appearance of NEP-B78 and an LBR-like protein during *Xenopus* nuclear envelope reassembly reflect the ordered recruitment of functionally discrete vesicle types. *J. Cell Biol.* 144:225–240.

Ellenberg, J., E.D. Siggia, J.E. Moreira, C.L. Smith, J.F. Presley, H.J. Worman, and J. Lippincott-Schwartz. 1997. Nuclear membrane dynamics and reassembly in living cells: targeting of an inner nuclear membrane protein in interphase and mitosis. *J. Cell Biol.* 138:1193–1206.

Ellis, D.J., H. Jenkins, W.G. Whitfield, and C.J. Hutchison. 1997. GST-lamin fusion proteins act as dominant negative mutants in *Xenopus* egg extract and reveal the function of the lamina in DNA replication. *J. Cell Sci.* 110:2507–2518.

Evan, G.I., G.K. Lewis, G. Ramsay, and J.M. Bishop. 1985. Isolation of monoclonal antibodies specific for human c-myc proto-oncogene product. *Mol. Cell. Biol.* 5:3610–3616.

Firmbach-Kraft, I., and R. Stick. 1993. The role of CaaX-dependent modifications in membrane association of *Xenopus* nuclear lamin B3 during meiosis and the fate of B3 in transfected mitotic cells. *J. Cell Biol.* 123:1661–1670.

Firmbach-Kraft, I., and R. Stick. 1995. Analysis of nuclear lamin isoprenylation in *Xenopus* oocytes: isoprenylation of lamin B3 precedes its uptake into the nucleus. *J. Cell Biol.* 129:17–24.

Fisher, D.Z., N. Chaudhary, and G. Blobel. 1986. cDNA sequencing of nuclear lamins A and C reveals primary and secondary structural homology to intermediate filament proteins. *Proc. Natl. Acad. Sci. USA.* 83:6450–6454.

Foisner, R. 1997. Dynamic organisation of intermediate filaments and associated proteins during the cell cycle. *Bioessays.* 4:297–305.

Frangioni, J.V., and B.G. Neel. 1993. Use of a general purpose mammalian expression vector for studying intracellular protein targeting: identification of critical residues in the nuclear lamin A/C nuclear localization signal. *J. Cell Sci.* 105:481–488.

Gajewski, A., and G. Krohne. 1999. Subcellular distribution of the *Xenopus* p58/lamin B receptor in oocytes and eggs. *J. Cell Sci.* 112:2583–2596.

Gant, T.M., and K.L. Wilson. 1997. Nuclear assembly. *Annu. Rev. Cell. Dev. Biol.* 13:669–695.

Gant, T.M., C.A. Harris, and K.L. Wilson. 1999. Roles of LAP2 proteins in nuclear assembly and DNA replication: truncated LAP2beta proteins alter lamina assembly, envelope formation, nuclear size, and DNA replication efficiency in *Xenopus laevis* extracts. *J. Cell Biol.* 144:1083–1096.

Georgatos, S.D., A. Pyrpasopoulou, and P.A. Theodoropoulos. 1997. Nuclear envelope breakdown in mammalian cells involves stepwise lamina disassembly and microtubule-driven deformation of the nuclear membrane. *J. Cell Sci.* 110:2129–2140.

Gerace, L., and G. Blobel. 1980. The nuclear envelope lamina is reversibly depolymerized during mitosis. *Cell.* 19:277–287.

Gerace, L., C. Comeau, and M. Benson. 1984. Organization and modulation of nuclear lamina structure. *J. Cell Sci. Suppl.* 1:137–160.

Glass, C.A., J.R. Glass, H. Taniura, K.W. Hasel, J.M. Blevitt, and L. Gerace. 1993. The alpha-helical rod domain of human lamins A and C contains a chromatin binding site. *EMBO (Eur. Mol. Biol. Organ.) J.* 12:4413–4424.

Goldman, A.E., R. D. Moir, M. Montag-Lowy, M. Stewart, and R.D. Goldman. 1992. Pathway of incorporation of microinjected lamin A into the nuclear envelope. *J. Cell Biol.* 119:725–735.

Haraguchi, T., T. Koujin, T. Hayakawa, T. Kaneda, C. Tsutsumi, N. Imamoto, C. Akazawa, J. Sukegawa, Y. Yoneda, and Y. Hiraoka. 2000. Live fluorescence imaging reveals early recruitment of emerin, LBR, RanBP2, and Nup153 to reforming functional nuclear envelopes. *J. Cell Sci.* 113:779–794.

Heim, R., and R.Y. Tsien. 1996. Engineering green fluorescent protein for improved brightness, longer wavelengths and fluorescence resonance energy transfer. *Curr. Biol.* 6:178–182.

Heitlinger, E., M. Peter, A. Lustig, W. Villiger, E.A. Nigg, and U. Aebi. 1992. The role of the head and tail domain in lamin structure and assembly: analysis of bacterially expressed chicken lamin A and truncated B2 lamins. *J. Struct. Biol.* 108:74–89.

Hennekes, H., and E.A. Nigg. 1994. The role of isoprenylation in membrane attachment of nuclear lamins. A single point mutation prevents proteolytic cleavage of the lamin A precursor and confers membrane binding properties. *J. Cell Sci.* 107:1019–1029.

Hoger, T.H., K. Zatloukal, I. Waizenegger, and G. Krohne. 1990. Characterization of a second highly conserved B-type lamin present in cells previously thought to contain only a single B-type lamin. *Chromosoma.* 99:379–390.

Hoger, T.H., G. Krohne, and J.A. Kleinschmidt. 1991. Interaction of *Xenopus* lamins A and LII with chromatin in vitro mediated by a sequence element in the carboxyterminal domain. *Exp. Cell Res.* 197:280–289.

Holtz, D., R.A. Tanaka, J. Hartwig, and F. McKeon. 1989. The CaaX motif of lamin A functions in conjunction with the nuclear localization signal to target assembly to the nuclear envelope. *Cell.* 59:969–977.

Hozak, P., A.M. Sasseville, Y. Raymond, and P.R. Cook. 1995. Lamin proteins form an internal nucleoskeleton as well as a peripheral lamina in human cells. *J. Cell Sci.* 108:635–644.

Hozak, P. 1996. The nucleoskeleton and attached activities. *Exp. Cell Res.* 229: 267–271.

Jones, J.C., A.E. Goldman, P.M. Steinert, S. Yuspa, and R.D. Goldman. 1982. Dynamic aspects of the supramolecular organization of intermediate filament networks in cultured epidermal cells. *Cell Motil.* 2:197–213.

Kilic, F., D.A. Johnson, and M. Sinensky. 1999. Subcellular localization and partial purification of prelamin A endoprotease: an enzyme which catalyzes the conversion of farnesylated prelamin A to mature lamin. *FEBS Lett.* 450: 61–65.

Kitten, G.T., and E.A. Nigg. 1991. The CaaX motif is required for isoprenylation, carboxyl methylation, and nuclear membrane association of lamin B2. *J. Cell Biol.* 113:13–23.

Lenz-Bohme, B., J. Wismar, S. Fuchs, R. Reifegerste, E. Buchner, H. Betz, and B. Schmitt. 1997. Insertional mutation of the *Drosophila* nuclear lamin Dm0 gene results in defective nuclear envelopes, clustering of nuclear pore complexes, and accumulation of annulate lamellae. *J. Cell Biol.* 137:1001–1016.

Lin, F., D.L. Blake, I. Callebaut, I.S. Skerjanc, L. Holmer, M.W. McBurney, M. Paulin-Levasseur, and H.J. Worman. 2000. MAN1, an inner nuclear membrane protein that shares the LEM domain with lamina-associated polypeptide 2 and emerin. *J. Biol Chem.* 275:4840–4847.

Loewinger, L., and F. McKeon. 1988. Mutations in the nuclear lamin proteins resulting in their aberrant assembly in the cytoplasm. *EMBO (Eur. Mol. Biol. Organ.) J.* 7:2301–2309.

Lourim, D., and G. Krohne. 1993a. Membrane-associated lamins in *Xenopus* egg extracts: identification of two vesicle populations. *J. Cell Biol.* 123:501–512.

Lourim, D., and G. Krohne. 1993b. Lamin-dependent nuclear envelope reassembly following mitosis: an argument. *Trends Cell Biol.* 4:315–317.

Maison, C., A. Pyrpasopoulou, P.A. Theodoropoulos, and S. Georgatos. 1997. The inner nuclear membrane protein LAP1 forms a native complex with B-type lamins and partitions with spindle-associated mitotic vesicles. *EMBO (Eur. Mol. Biol. Organ.) J.* 16:4839–4850.

McKeon, F.D., M.W. Kirschner, and D. Caput. 1986. Homologies in both primary and secondary structure between nuclear envelope and intermediate filament proteins. *Nature.* 319:463–468.

Meier, J., K.H. Campbell, C.C. Ford, R. Stick, and C.J. Hutchison. 1991. The role of lamin LIII in nuclear assembly and DNA replication, in cell-free extracts of *Xenopus* eggs. *J. Cell Sci.* 98:271–279.

Meier, J., and S.D. Georgatos. 1994. Type B lamins remain associated with the integral nuclear envelope protein p58 during mitosis: implications for nuclear reassembly. *EMBO (Eur. Mol. Biol. Organ.) J.* 13:1888–1898.

Mical, T.I., and M.J. Monteiro. 1998. The role of sequences unique to nuclear intermediate filaments in the targeting and assembly of human lamin B: evidence for lack of interaction of lamin B with its putative receptor. *J. Cell Sci.* 111:3471–3485.

Moir, R.D., A.D. Donaldson, and M. Stewart. 1991. Expression in *Escherichia*

coli of human lamins A and C: influence of head and tail domains on assembly properties and paracrystal formation. *J. Cell Sci.* 99:363–372.
Moir, R.D., M. Montag-Lowy, and R.D. Goldman. 1994. Dynamic properties of nuclear lamins: lamin B is associated with sites of DNA replication. *J. Cell Biol.* 125:1201–1212.
Moir R.D, T.P. Spann, and R.D. Goldman. 1995. The dynamic properties and possible functions of nuclear lamins. *Int. Rev. Cytol.* 162B:141–182.
Moir, R.D., T.P. Spann, H. Herrmann, and R.D. Goldman. 2000. Disruption of nuclear lamin organization blocks the elongation phase of DNA replication. *J. Cell Biol.* 149:1179–1192.
Neri, L.M., Y. Raymond, A. Giordano, S. Capitani, and A.M. Martelli. 1999. Lamin A is part of the internal nucleoskeleton of human erythroleukemia cells. *J. Cell Physiol.* 78:284–295.
Newport, J.W., K. L. Wilson, and W.G. Dunphy. 1990. A lamin-independent pathway for nuclear envelope assembly. *J. Cell Biol.* 111:2247–2259.
Pederson, T. 1998. Thinking about a nuclear matrix. *J. Mol. Biol.* 277:147–159.
Pederson, T. 2000a. Half a century of "the nuclear matrix." *Mol. Biol. Cell.* 11: 799–805.
Pederson, T. 2000b. Diffusional protein transport within the nucleus: a message in the medium. *Nat. Cell Biol.* 2:E73–E74.
Peter, M., E. Heitlinger, M. Haner, U. Aebi, and E.A. Nigg. 1991. Disassembly of in vitro formed lamin head-to-tail polymers by CDC2 kinase. *EMBO (Eur. Mol. Biol. Organ.) J.* 10:1535–1544.
Pollard, K.M., E.K. Chan, B.J. Grant, K.F. Sullivan, E.M. Tan, and C.A. Glass. 1990. In vitro posttranslational modification of lamin B cloned from a human T-cell line. *Mol. Cell. Biol.* 10:2164–2175.
Rober, R.A., K. Weber, and M. Osborn. 1989. Differential timing of nuclear lamin A/C expression in the various organs of the mouse embryo and the young animal: a developmental study. *Development (Camb.).* 105:365–378.
Sasseville, A., and Y. Raymond. 1995. Lamin A precursor is localized to intranuclear foci. *J. Cell Sci.* 108:273–285.
Spann, T.P., R.D. Moir, A.E. Goldman, R. Stick, and R.D. Goldman. 1997. Disruption of nuclear lamin organization alters the distribution of replication factors and inhibits DNA synthesis. *J. Cell Biol.* 136:1201–1212.
Stewart, C., and B. Burke. 1987. Teratocarcinoma stem cells and early mouse embryos contain only a single major lamin polypeptide closely resembling lamin B. *Cell.* 51:383–392.
Stuurman, N., S. Heins, and U. Aebi. 1998. Nuclear lamins: their structure, assembly, and interactions. *J. Struct. Biol.* 122:42–66.
Ulitzur, N., A. Harel, N. Feinstein, and Y. Gruenbaum. 1992. Lamin activity is essential for nuclear envelope assembly in a *Drosophila* embryo cell-free extract. *J. Cell Biol.* 119:17–25.
Ulitzur, N., A. Harel, M. Goldberg, N. Feinstein, and Y. Gruenbaum. 1997. Nuclear membrane vesicle targeting to chromatin in a *Drosophila* embryo cell-free system. *Mol. Biol. Cell.* 8:1439–1448.
Vickstrom, K.L., S.S. Lim, R.D. Goldman, and G.G. Borisy. 1992. Steady state dynamics of intermediate filament networks. *J. Cell Biol.* 118:121–129l
Vigers, G.P., and M. Lohka. 1991. A distinct vesicle population targets membranes and pore complexes to the nuclear envelope in *Xenopus* eggs. *J. Cell Biol.* 112:545–556.
Vlcek, S., H. Just, T. Dechat, and R. Foisner. 1999. Functional diversity of LAP2alpha and LAP2beta in postmitotic chromosome association is caused by an alpha-specific nuclear targeting domain. *EMBO (Eur. Mol. Biol. Organ.) J.* 18:6370–6384.
Vorburger, K., G.T. Kitten, and E.A. Nigg. 1989. Modification of nuclear lamin proteins by a mevalonic acid derivative occurs in reticulocyte lysates and requires the cysteine residue of the C-terminal CXXM motif. *EMBO (Eur. Mol. Biol. Organ) J.* 8:4007–4013.
Weber, K., U. Plessmann, and P. Traub. 1989. Maturation of nuclear lamin A involves a specific carboxy-terminal trimming, which removes the polyisoprenylation site from the precursor: implications for the structure of the nuclear lamina. *FEBS Lett.* 257:411–414.
Wiese, C., M.W. Goldberg, T.D. Allen, and K.L.Wilson. 1997. Nuclear envelope assembly in *Xenopus* extracts visualized by scanning EM reveals a transport-dependent envelope smoothing event. *J. Cell Sci.* 110:1489–1502.
Yang, L., T. Guan, and L. Gerace. 1997. Integral membrane proteins of the nuclear envelope are dispersed throughout the endoplasmic reticulum during mitosis. *J. Cell Biol.* 137:1199–1210.
Yoon, M., R.D. Moir, V. Prahlad, and R.D. Goldman. 1998. Motile properties of vimentin intermediate filament networks in living cells. *J. Cell Biol.* 143: 147–157.
Zewe, M., T.H. Hoger, T. Fink, P. Lichter, G. Krohne, and W.W. Franke. 1991. Gene structure and chromosomal localization of the murine lamin B2 gene. *Eur. J. Cell Biol.* 56:342–350.